Received: 18 July 2020 | Revised: 30 October 2020 | Accepted: 2 November 2020

DOI: 10.1002/jcla.23653

RESEARCH ARTICLE

WILEY

iTRAQ-based proteomic analysis of the molecular mechanisms and downstream effects of fatty acid synthase in osteosarcoma cells

Dahua Fu[1] | Shuochuan Liu[2] | Jiaming Liu[3,4] | Wenzhao Chen[3] | Xinhua Long[5] | Xuanyin Chen[3] | Yang Zhou[3] | Yibin Zheng[3] | Shanhu Huang[3]

[1]Department of Pharmacy, Zhangzhou health vocational college, Zhangzhou, China

[2]Queen Mary school, Nanchang University, Nanchang, China

[3]Department of Orthopedic Surgery, The First Affiliated Hospital of Nanchang University, Nanchang, China

[4]Jiangxi Institute of Respiratory Disease, The First Affiliated Hospital of Nanchang University, Nanchang, China

[5]Department of Emergency Surgery, The First Affiliated Hospital of Nanchang University, Nanchang, China

Correspondence
Shanhu Huang, Department of Orthopedic Surgery, the First Affiliated Hospital of Nanchang University, No. 17 Yong Wai Zheng Street, Donghu District, Nanchang, Jiangxi Province, China.
Email: hsh869@126.com

Funding information
This study was supported by the National Natural Science Foundation of China (No. 81660442, 81860472, and 81560435).

Abstract

Background: Fatty acid synthase (FASN) is a lipogenic enzyme that participates in tumor progression. We previously showed that FASN is dysregulated in OS malignancy, but the molecular mechanism(s) of these effects remained unclear.

Methods: We examined differentially expressed proteins (DEPs) in FASN-silenced osteosarcoma 143B cells and their parental cells by isobaric tags for relative and absolute quantitation (iTRAQ). Differentially expressed proteins were classified using GO and KEGG analysis. The association between FASN and heterogeneous nuclear ribonucleoprotein A1 (HNRNPA1) was confirmed using qPCR, Western blot, and immunohistochemistry. The function of HNRNPA1 in osteosarcoma was determined using CCK-8, colony formation, wound healing, transwell migration, and invasion assays.

Results: Among the 4971 identified proteins, 567 DEPs (325 upregulated and 242 downregulated) were identified. The top 10 upregulated proteins comprised HIST1H2AB, INA, INTS5, MTCH2, EIF1, MAPK1IP1L, PXK, RPS27, PM20D2, and ZNF800, while the top 10 downregulated proteins comprised NDRG1, CNTLN, STON2, GDF7, HECTD3, HBB, TPM1, PPP4R4, PTTG1IP, and PLCB3. Bioinformatic analysis indicated that the DEPs were related to cellular processes, metabolic processes, biological regulation, binding, and catalytic activity. HNRNPA1 was dysregulated in FASN-silenced 143B and HOS cells. qPCR, Western blot, and immunohistochemistry showed that FASN expression positively correlates with HNRNPA1 expression. Further studies indicated that HNRNPA1 correlates with OS diagnosis and prognosis. And HNRNPA1 silence inhibits the proliferation, migration, and invasion in OS cells.

Conclusion: HNRNPA1 acts as targets downstream of FASN and potential biomarker and oncogene in OS.

KEYWORDS
FASN, HNRNPA1, iTRAQ proteomic analysis, osteosarcoma

Dahua Fu and Shuochuan Liu contributed equally to this work.

1 | INTRODUCTION

Osteosarcoma (OS) is the most common solid tumor in adolescences and the elderly.[1] OS is a highly aggressive tumor that frequently metastasizes to the lungs. In the 1970s, the introduction of multiple chemotherapeutic drug regimens led to a significant breakthrough in OS treatment and improved 5-year survival rates of OS patients from 20% to close to 70%.[2,3] Although many treatments for primary and advanced osteosarcomas have been developed,[4] the overall progress in OS treatment is limited over the past 30 years, and new therapeutic targets for OS treatment are urgently required.

Fatty acid synthase (FASN) is an enzymatic system consisting of two identical multifunctional polypeptides, the primary functions of which are to catalyze the synthesis of long-chain fatty acids.[5,6] FASN has been identified as an oncogene and potential prognostic biomarker in gastric adenocarcinoma[7] and breast cancer.[8] Emerging evidence demonstrated that FASN is associated with cell proliferation, migration, apoptosis, and radiosensitivity.[9-11] Our previous studies also showed that FASN enhances the migration and invasion of OS cells via PI3K/Akt signaling pathway.[12] However, a detailed evaluation of FASN functionality in OS has not been performed. iTRAQ-based proteomic analysis reveals changes in intracellular protein expression and protein-protein networks to improve our understanding of protein functionality.

In this study, we used iTRAQ-based proteomic analysis to investigate the impact of FASN knockdown in OS cells. Protein expression profiling revealed 526 DEPs in FASN knockdown groups. Functional annotation clustering using gene ontology (GO) and Kyoto Encyclopedia of Genes and Genomes (KEGG) analysis revealed that the DEPs belonged to functional pathways including cellular processes, metabolic processes, biological regulation, binding, and catalytic activity. Bioinformatic analysis revealed that HNRNPA1 expression was positively associated with FASN expression and predicted a poor prognosis in OS patients, which was also confirmed in OS cells and tissues in this study. Finally, we found that HNRNPA1 was upregulated in OS cell lines and HNRNPA1 silence inhibited the proliferation and migration in OS cells. These findings highlight HNRNPA1 as a biomarker of OS and the FASN/HNRNPA1 axis as a novel molecular target for OS therapeutics.

2 | MATERIALS AND METHODS

2.1 | Tissue specimens and patients

Clinically diagnosed OS samples (n = 71) were obtained from the First Affiliated Hospital of Nanchang University, China. FASN and HNRNPA1 expressions were determined by IHC staining. IHC scores were based on the percentage of positively stained cells (0:0%, 1: <25%, 2:25% ~ 50%, 3:50% ~ 75%, and 4: ≥75%) and color intensity (0: negative, 1: weak, 2: medium, and 3: strong). Scores were calculated by multiplying the intensity and positivity, ranging from 0 to 12. Score <4 was defined as "-", score 4 was defined as "+", scores 6 and 8 were defined as "++", and score 12 was defined as "+++". The clinical parameters of OS patients with low or high HNRNPA1 expression are shown in Table 1. Kaplan-Meier analysis was performed to compare the overall survival of low and high HNRNPA1 expression patients. Follow-up information of 11 OS patients was lost. The ethics committee of the First Affiliated Hospital of Nanchang University approved the study. And all the subjects were informed of the contents, latent risks, objectives, and signed written informed consents.

TABLE 1 Correlation of HNRNPA1 protein expression in OS tissues with clinical pathologic parameters

Variables	All cases	HNRNPA1 expression		p-value
		Low	High	
Gender				
Male	41	19 (46.3%)	22 (53.7%)	0.337
Female	30	18 (60%)	12 (40%)	
Age				
≤20	35	19 (54.2%)	16 (45.8%)	0.814
>20	36	18 (50%)	18 (50%)	
Location				
Femur/tibia	54	27 (50%)	27 (50%)	0.586
Elsewhere	17	10 (58.8%)	7 (41.2%)	
Tumor size (cm)				
≤5	23	16 (69.6%)	7 (30.4%)	0.047*
>5	48	21 (43.8%)	27 (56.2%)	
Distant metastasis				
No	52	32 (61.5%)	20 (38.5%)	0.015*
Yes	19	5 (26.3%)	14 (73.7%)	
Enneking staging				
I+IIA	40	26 (65%)	14 (35%)	0.017*
IIB+III	31	11 (35.5%)	20 (64.5%)	

Note: p-value was calculated by Pearson's chi-square test.
*$p < 0.05$.

2.2 | Bioinformatic analysis

The R2 database (http://hgserver1.amc.nl) was used to investigate the correlation between FASN and relative gene expressions in 127 mixed OS samples. Kaplan-Meier survival curves were generated to investigate the relationship between relative gene expression and OS prognosis. Follow-up information of 39 OS patients was lost.

2.3 | Cell culture and transfection

The human osteoblast cell line hFOB1.19 and osteosarcoma cell lines 143B, HOS, and U2OS were purchased from the Chinese Academy of Science (Shanghai, China) and authenticated by STR profiling. hFOB1.19 cells were maintained in DMEM/F12 culture medium,

and 143B, HOS, and U2OS cells were maintained in DMEM (Gibco, Carlsbad, CA, USA), all supplemented with 10% FBS (Gibco). For the transfections, 10^4 cells were plated into 6-well plates and treated with the indicated lentiviruses (MOI = 100) following the manufacturer's instructions. Cells were incubated for 24 h and then rinsed twice with phosphate buffer, followed by incubation with DMEM containing 0.8 mg/ml puromycin to select stably transfected cells. Short hairpin RNAs (shRNA) were used to knockdown FASN and HNRNPA1 expression. The sequences are listed in Table 2.

2.4 | RNA isolation and quantitative real-time PCR

qRT-PCR analysis was performed according to previously described procedures.[13] Primer sequences are shown in Table 2.

2.5 | Western blot

Cells were lysed in RIPA buffer, and total protein concentrations of cell lysate were measured via BCA assays (Thermo Fisher Scientific, Main St, MA, USA) according to the manufacturer's instructions. A certain amount of proteins were denatured, subjected to 10% ~ 12% SDS-PAGE, and then transferred to PVDF membranes (Millipore, Darmstadt, Germany). Blocked with 5% skimmed milk (BD Biosciences, San Jose, CA, USA), membranes were incubated with anti-FASN (CST, 3180), anti-HNRNPA1 (Origene, TA314018), or anti-GAPDH (Origene, TA802519) primary antibodies for 12 h at 4°C. After washed three times with TBST, membranes were incubated with HRP-conjugated anti-rabbit (Abcam) or anti-mouse (Abcam) secondary antibodies for 1 h at room temperature. Protein band detection was performed by using ECL Prime Western Blotting Reagent (Amersham Biosciences, Piscataway, NJ, USA) and visualized using the digital gel image analysis system (Tanon, Japan).

2.6 | Cell proliferation and colony formation assay

The Cell Counting Kit-8 (CCK-8) assay was performed to assess the cell viability. In brief, human osteosarcoma 143B or HOS cells were seeded in 96-well plates at an optimal density. After the aforementioned treatments, cells were incubated with CCK-8 reagent (Dojindo Laboratories, Kumamoto, Japan) at 37°C for 2 h. The optical density of samples at 24 h, 48 h, 72 h, and 96 h, respectively, was detected by using a microplate reader at a wavelength of 450 nm. For colony formation assay, 1500 143B or HOS cells were seeded into 6-well plates, after an inclusive culture for 8 days. Cells were incubated with PFA (4%) and stained with crystal violet (2.5%).

2.7 | Wound-healing scratch assay

5×10^6 143B and HOS cells were seeded into six-well plates and grown to 90% confluency. Scratch assays were performed with a 10-μl pipette tip. Cells were then incubated with DMEM containing 20% FBS. Images were captured at 0 h and 24 h, respectively, after wounding, and cell migration distances between the front lines were measured by ImageJ software.

2.8 | Transwell assays

5×10^5 cells were suspended in 200 μl serum-free medium and seeded in the upper chamber (Millipore) pre-coated with or without Matrigel (1:8 dilution; BD). The lower chambers were supplemented with 500 μl complete medium. 24 h later, the chambers were harvested and the cotton swabs were used to remove the remaining Matrigel and cells in the upper chamber. Cells were fixed by PFA (4%) and subsequently stained with 2.5% crystal violet. Cells in five microscopic fields were counted and photographed.

TABLE 2 Primer sequences

Primer sequences for qRT-PCR		
Name	**Forward (5′→3′)**	**Reverse (5′→3′)**
FASN	CAACTCACGCTCCGGAAA	TGTGGATGCTGTCAAGGG
HNRNPA1	ACGAAACCAAGGTGGCTATG	GTGCTTGGCTGAGTTCACAA
UBA52	GCCTGCGAGGTGGCATTATTGA	TTCTTGCGGCAGTTGACAGCAC
RPS27	AAGAAACGCCTGGTGCAGAGCC	TGTAGGCTGGCAGAGGACAGTG
RPS9	GTCTCGACCAAGAGCTGAAGCT	GGTCCTTCTCATCAAGCGTCAG
RPS28	AAAGGCTGAGGTGACTGACG	CACGTTTCCTGCCTCAAGGA
RPS18	GCAGAATCCACGCCAGTACAAG	GCTTGTTGTCCAGACCATTGGC
GADPH	CCACCCATGGCAAATTCCATGGCA	TCTAGACGGCAGGTCAGGTCCACC
Primer sequences for shRNA		
Name		
shFASN	CCTGCGTGGCCTTTGAAATGTCTCGAGACATTTCAAAGGCCACGCAGG	
shHNRNPA1	GCCACAACTGTGAAGTTAGAACTCGAGTTCTAACTTCACAGTTGTGGCTTTTT	

2.9 | Protein preparation, digestion, and iTRAQ labeling

Briefly, 10^7 143B cells were lysed using SDT buffer (4% (w/v) SDS, 0.1 M DTT, 100 mM Tris/HCL (pH 7.6). Proteins were hydrolyzed with trypsin (FASP), and resulting peptides were quantified at 280 nm. Peptide segments (100 μg) were then iTRAQ-labeled for further analysis.

2.10 | Peptide fractionation with high pH reversed phase

Labeled peptides were mixed in equal amounts of buffer and graded by using high pH Reversed-phase Peptide Fractionation Kits. Firstly, columns were equilibrated with acetonitrile and 0.1% trifluoroacetic acid (TFA) before loading. Then, desalted mixed labeled peptides were pumped to the column. Finally, elution was performed by using a linear gradient of high pH acetonitrile. Fractions were collected and lyophilized. The dry samples were redissolved in 12 μl of 0.1% formic acid (FA).

2.11 | LC-MS/MS data acquisition

Samples were redissolved by using nanometric flow. Buffer A consisted of 0.1% formic acid aqueous solution, while buffer B consisted of 0.1% formic acid aqueous solution and acetonitrile (16%:84%). Chromatographic columns were balanced with solution of 95% buffer A. Samples were injected automatically into the sample column (Thermo Scientific Acclaim PepMap 100, 100 μm × 2 cm, nanoViper C18) and separated by liquid chromatography (Thermo Scientific EASY Column, 10 cm, ID75 μm, C18-A2) at a flow rate of 300 nl/min, coupled with detection by positive-ion electrospray ionization mass spectrometry. The mass-to-charge ratio of the peptides and polypeptide fragments were collected from 20 fragments (MS2 scan) after each full scan.

2.12 | Data analysis

LC-MS/MS spectra were processed and identified using the MASCOT engine (Matrix Science, London, UK; version 2.2) and Proteome Discoverer (Thermo Fisher Scientific; version 1.4). The parameters used to identify the proteins were listed as follows: max missed cleavages = 2; fixed modifications = carbamidomethyl (C), TMT 6/10 plex (N term), TMT6/10 plex (K); variable modifications = oxidation (M), TMT 6/10plex (Y), peptide mass tolerance = ±20 ppm; and fragment mass tolerance = 0.1 Da. Proteins were searched using the SwissProt Human database with the target-decoy database pattern. Protein ratios were processed as the median of the unique peptides of the protein. Peptide ratios were normalized using the median protein ratio (median protein ratio = 1).

2.13 | Bioinformatic analysis

Proteins were loaded onto Blast2GO (version 5.2.5) for Gene Ontology annotations. The KASS (KEGG Automatic Annotation Server) program was used to blast and annotate target proteins. Enrichment analysis of whole DEPs was processed by using Fisher's exact test. Heat maps were generated using the Complex Heat map R (R version 3.4) after the classification of expression of samples and proteins in two dimensions. Protein-protein interactions (PPIs) were searched, and networks were generated by using String (https://string-db.org/). Cytoscape (Version: 3.2.1) was used to generate networks.

2.14 | Statistical analysis

Gene Expression Omnibus (GEO) data were analyzed by using non-parametric Wilcoxon rank-sum test analysis. All continuous data were presented as the mean ± standard deviation. Student's *t*-test was used for the comparison of two samples. Multiple samples were analyzed via a one-way ANOVA $p < 0.05$ was considered to indicate a statistically significant difference. All analyses were performed by using SPSS statistical software version 13.0 (SPSS, IBM Corporation, Armonk, NY, USA).

3 | RESULTS

3.1 | Global protein profiling in FASN-silenced OS cells

Lysates from cells stably transfected with LV/shFASN or LV/shNC were analyzed using high-accuracy LC/MS/MS iTRAQ analysis combined with SCX. Each group consisted of three parallel samples. Differentially expressed proteins were defined as a 1.2-fold change. *p*-values ≤ 0.05 were assessed as previously described.[14] Among the 4971 quantified proteins, a total of 567 DEPs (325 upregulated, 242 downregulated) were identified. Protein ratio distributions are shown in Figure 1A. Volcano plots and heat maps were constructed to analyze the significance and magnitude of the quantitative DEP data (Figure 1B,C). Representative DEPs are listed in Table 3.

3.2 | Gene ontology enrichment analysis

To further understand the biological changes in FASN-silenced OS cells, identified DEPs were analyzed by GO analysis. DEPs were classified into three categories: biological processes (BPs), molecular functions (MFs), and cellular components (CCs). GO biological processes (BPs) were mainly related to metabolic processes, cellular processes, the regulation of biological processes, biological regulation, and cellular component organization or biogenesis. The GO molecular function (MF) terms were related to binding, catalytic activity, structural molecular activity, transcription regulator activity,

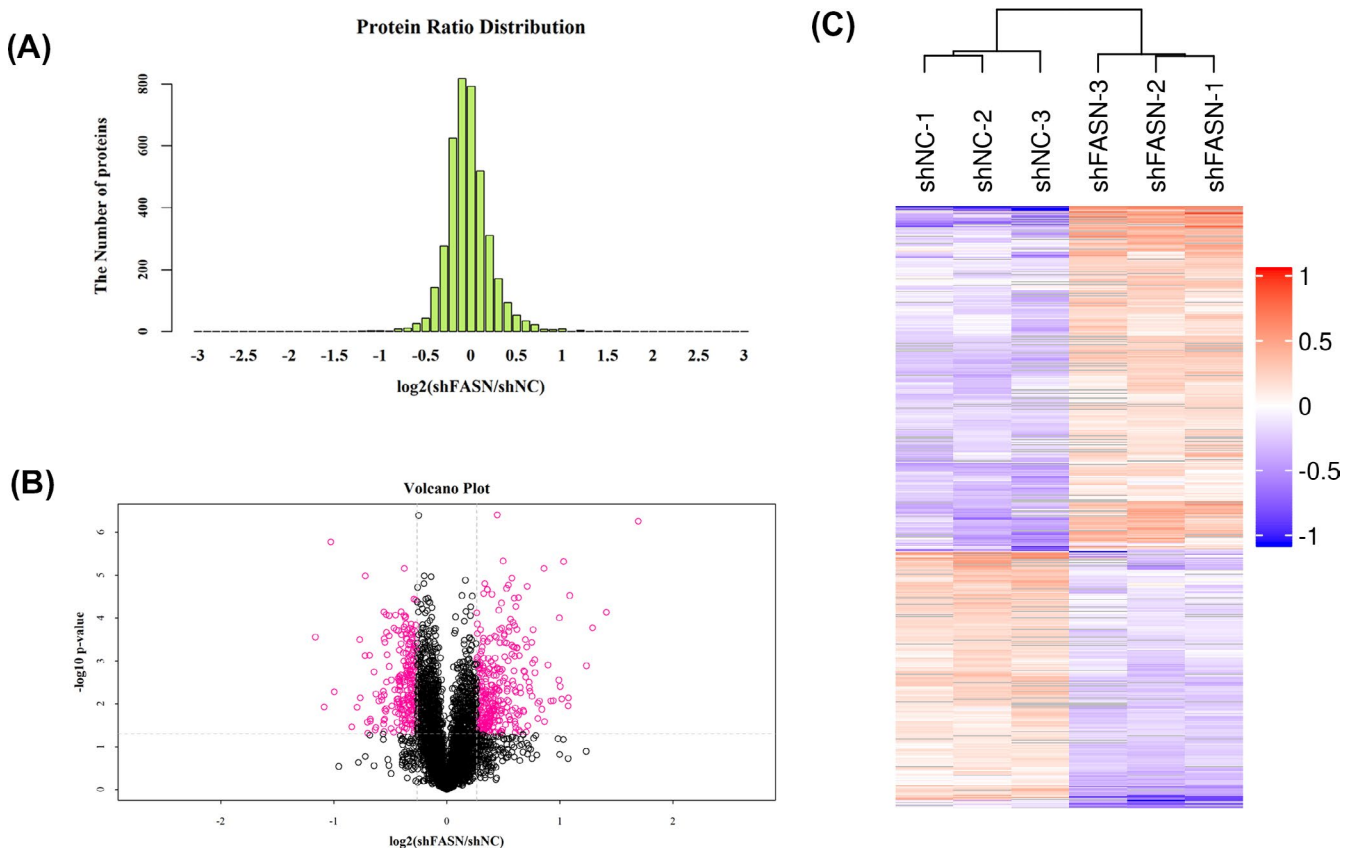

FIGURE 1 Global protein profiling in FASN-silenced OS cells. A, Protein ratio distribution in FASN-silenced and control groups. The Abscissa represents the fold change in identified DEPs, and longitudinal coordinates represent the number of identified DEPs. Heat maps (B) and volcano plot (C) analysis of the DEPs. Gray: no quantitative information. Green: downregulated proteins. Red: upregulated proteins

and molecular function regulator. GO cellular component (CC) terms were mainly related to cell parts, organelles, cells, organelle parts, and membranes (Figure 2A).

3.3 | KEGG analysis

Differentially expressed proteins were classified using the KEGG database to annotate the pathways associated with FASN expression. The top five pathways enriched in protein numbers were pathways in cancer, ribosomes, Huntington's disease, RNA transport, and thermogenesis (Figure 2B).

3.4 | Protein-protein interactions and network construction

The PPI network was constructed based on data from the String database (Figure S1). In this network, hub proteins including UBA52 (P62987, Ubiquitin-60S ribosomal protein L40, 83 degrees), RPS27 (P42677, 40S ribosomal protein S27, 43 degrees), RPS9 (P46781, ribosomal protein S9, 42 degrees), RPS28 (P62857, ribosomal protein S28, 40 degrees), and RPS18 (P62269, 40S ribosomal protein S18). The expressions of hub genes in FASN-silenced osteosarcoma cells were then validated by RT-PCR. As expected, the expressions of hub genes UBA52, RPS27, RPS9, and RPS18 were significantly downregulated in FASN-silenced 143B cells. The decrease with no significant difference in RPS28 expression was also observed (Figure S2). The result was consistent with the KEGG analysis, implicating FASN as an essential regulator of ribosome-related functions.

3.5 | Proteomic and bioinformatic analyses identified HNRNPA1 as a FASN-regulated protein

To investigate the potential downstream targets of FASN, we explored the R2 database (https://hgserver1.amc.nl/cgi-bin/r2/main.cgi) to investigate the correlation between FASN expression and the expression of the top 20 downregulated proteins (Lists 1-2). We further predicted the prognosis of candidate proteins in the R2 database (List 3). Finally, we examined the expression of the top 20 downregulated proteins in 18 OS and paired normal tissues using the GEO database (List 4). The results revealed that HNRNPA1 was the only common protein across the four lists (Figure 3A). Correlation analysis indicated that FASN expression was positively associated with HNRNPA1 expression (r = 0.528, p = 1.72e-10) (Figure 3B). HNRNPA1 expression was significantly

TABLE 3 Representative DEPs (>1.20-fold, $p < .05$) identified by iTRAQ proteomic analysis in FASN-silencing 143B cells

Protein IDs	Gene name	Protein name	Fold change	*p*-value
Upregulated DEPs				
P04908	HIST1H2AB	Histone H2A type 1-B/E	3.228901	5.53E-07
Q16352	INA	Alpha-internexin	2.657513	7.42E-05
Q6P9B9	INTS5	Integrator complex subunit 5	2.442719	0.000169616
Q9Y6C9	MTCH2	Mitochondrial carrier homolog 2	2.352293	0.001301533
P41567	EIF1	Eukaryotic translation initiation factor 1	2.123124	3.03E-05
Q8NDC0	MAPK1IP1L	MAPK-interacting and spindle-stabilizing protein-like	2.105968	0.007264445
Q7Z7A4	PXK	PX domain-containing protein kinase-like protein	2.101449	0.011252056
P42677	RPS27	40S ribosomal protein S27	2.045026	4.84E-06
Q8IYS1	PM20D2	Peptidase M20 domain-containing protein 2	2.021715	0.007757566
Q2TB10	ZNF800	Zinc finger protein 800	2.001644	0.003937428
Downregulated DEPs				
Q92597	NDRG1	Protein NDRG1	0.446553	0.000279489
Q9NXG0	CNTLN	Centlein	0.471089	0.011811997
Q8WXE9	STON2	Stonin-2	0.490429	1.70E-06
Q7Z4P5	GDF7	Growth/differentiation factor 7	0.501552	0.00525655
Q5T447	HECTD3	E3 ubiquitin-protein ligase HECTD3	0.557736	0.034490941
P68871	HBB	Hemoglobin subunit beta	0.576182	0.011936263
P09493	TPM1	Tropomyosin alpha-1 chain	0.585566	0.0003206
Q6NUP7	PPP4R4	Serine/threonine-protein phosphatase 4 regulatory subunit 4	0.588257	0.007326053
P53801	PTTG1IP	Pituitary tumor-transforming gene 1 protein-interacting protein	0.605621	0.00075919
Q01970	PLCB3	1-Phosphatidylinositol 4,5-bisphosphate phosphodiesterase beta-3	0.606634	1.05E-05

higher in OS ($p = 0.0139$) (Figure 3C), and the overexpression of HNRNPA1 was predictive of a poor prognosis ($n = 88$ OS patients, $p = 0.012$, Figure 3D). These data indicated that HNRNPA1 is a potential downstream target of FASN and promotes tumor development in OS.

3.6 | Validation of HNRNPA1 as a downstream target of FASN in OS cells and tissues

To further confirm above hypothesis, we examined mRNA and protein expression in the FASN knockdown cell lines 143B and HOS. RT-PCR data suggested that FASN knockdown led to decrease in HNRNPA1 expression at both the mRNA and protein level (Figure 4A,B). qRT-PCR and immunohistochemistry (IHC) assays were performed to investigate the correlation between FASN expression and HNRNPA1 expression in 71 clinical OS samples. Pearson's correlation analysis indicated that FASN protein level was positively related to HNRNPA1 protein level ($r = 0.4491$, $P < 0.0001$) (Figure 4C,D). In addition, we analyzed the association between HNRNPA1 expression and the clinical parameters of OS patients. We found that HNRNPA1 expression was positively correlated with distant metastasis, tumor size, and clinical stage (Table 1, Figure 4E). Kaplan-Meier analysis revealed that higher HNRNPA1 levels were related to a poor prognosis (Figure 4F). In conclusion, these data suggested that FASN regulates HNRNPA1 expression in both cell lines and tissues, and that HNRNPA1 may act as a novel biomarker for OS.

3.7 | HNRNPA1 silence inhibits proliferation, migration, and invasion in OS cells

Previous study has demonstrated that HNRNPA1 played an essential role in tumor progression,[15,16] but the expression and function of HNRNPA1 in osteosarcoma remained unclear. To clarify this, we detected the expression of HNRNPA1 in osteosarcoma cell lines. As shown in Figure 5A, HNRNPA1 expression was significantly higher in osteosarcoma cell lines 143B, HOS, and U2OS than in normal osteoblast cell line hFOB 1.19. To investigate whether HNRNPA1 was involved in OS malignancy, 143B and HOS cells were transfected with short hairpin RNA to downregulate HNANPA1 expression, and HNANPA1 knockdown efficiency was validated by qRT-PCR and

FIGURE 2 GO annotations and KEGG pathway enrichment analysis. A, DEPs were classified into three categories: biological processes (BP), molecular functions (MF), and cellular components (CC). B, KEGG analysis was performed using Fisher's exact test. The top 20 pathways affected by FASN silencing were listed

(A)

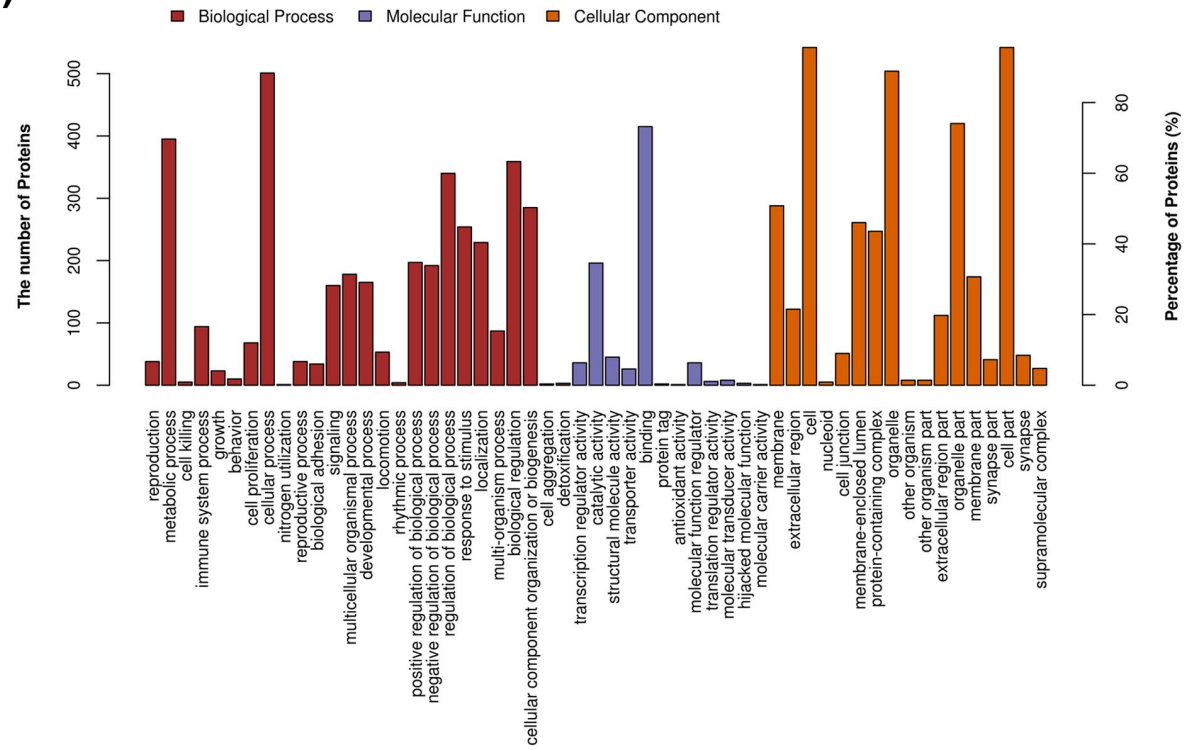
Biological Process
Molecular Function
Cellular Component
The number of Proteins
Percentage of Proteins (%)
0
100
200
300
400
500
0
20
40
60
80
reproduction
metabolic process
cell killing
immune system process
growth
behavior
cell proliferation
cellular process
nitrogen utilization
reproductive process
biological adhesion
signaling
multicellular organismal process
developmental process
locomotion
rhythmic process
positive regulation of biological process
negative regulation of biological process
regulation of biological process
response to stimulus
localization
multi-organism process
biological regulation
cellular component organization or biogenesis
cell aggregation
detoxification
transcription regulator activity
catalytic activity
structural molecule activity
transporter activity
binding
protein tag
antioxidant activity
molecular function regulator
translation regulator activity
molecular transducer activity
hijacked molecular function
molecular carrier activity
membrane
extracellular region
cell
nucleoid
cell junction
membrane-enclosed lumen
protein-containing complex
organelle
other organism
other organism part
extracellular region part
organelle part
membrane part
synapse part
cell part
synapse
supramolecular complex

(B)

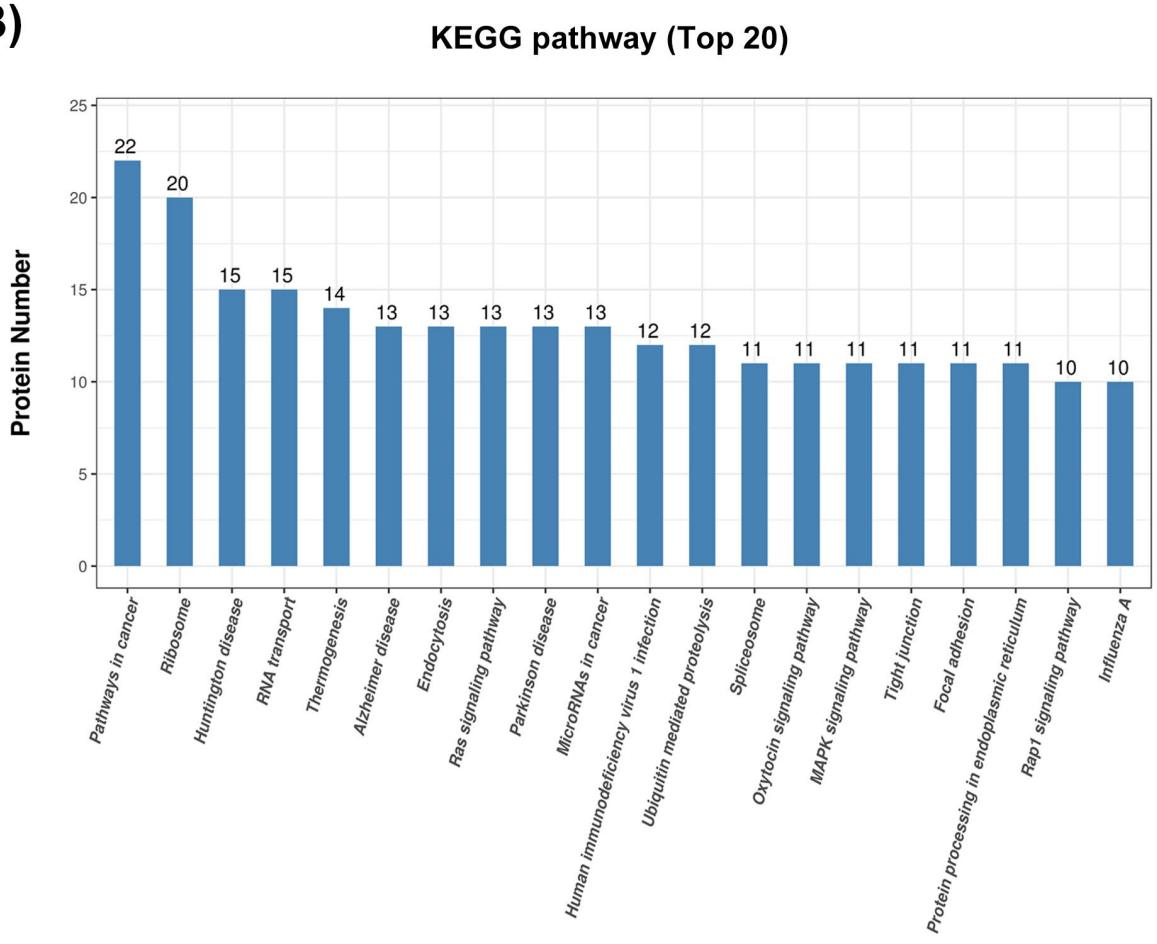
KEGG pathway (Top 20)
Protein Number
0
5
10
15
20
25
22
20
15
15
14
13
13
13
13
13
12
12
11
11
11
11
11
11
10
10
Pathways in cancer
Ribosome
Huntington disease
RNA transport
Thermogenesis
Alzheimer disease
Endocytosis
Ras signaling pathway
Parkinson disease
MicroRNAs in cancer
Human immunodeficiency virus 1 infection
Ubiquitin mediated proteolysis
Spliceosome
Oxytocin signaling pathway
MAPK signaling pathway
Tight junction
Focal adhesion
Protein processing in endoplasmic reticulum
Rap1 signaling pathway
Influenza A

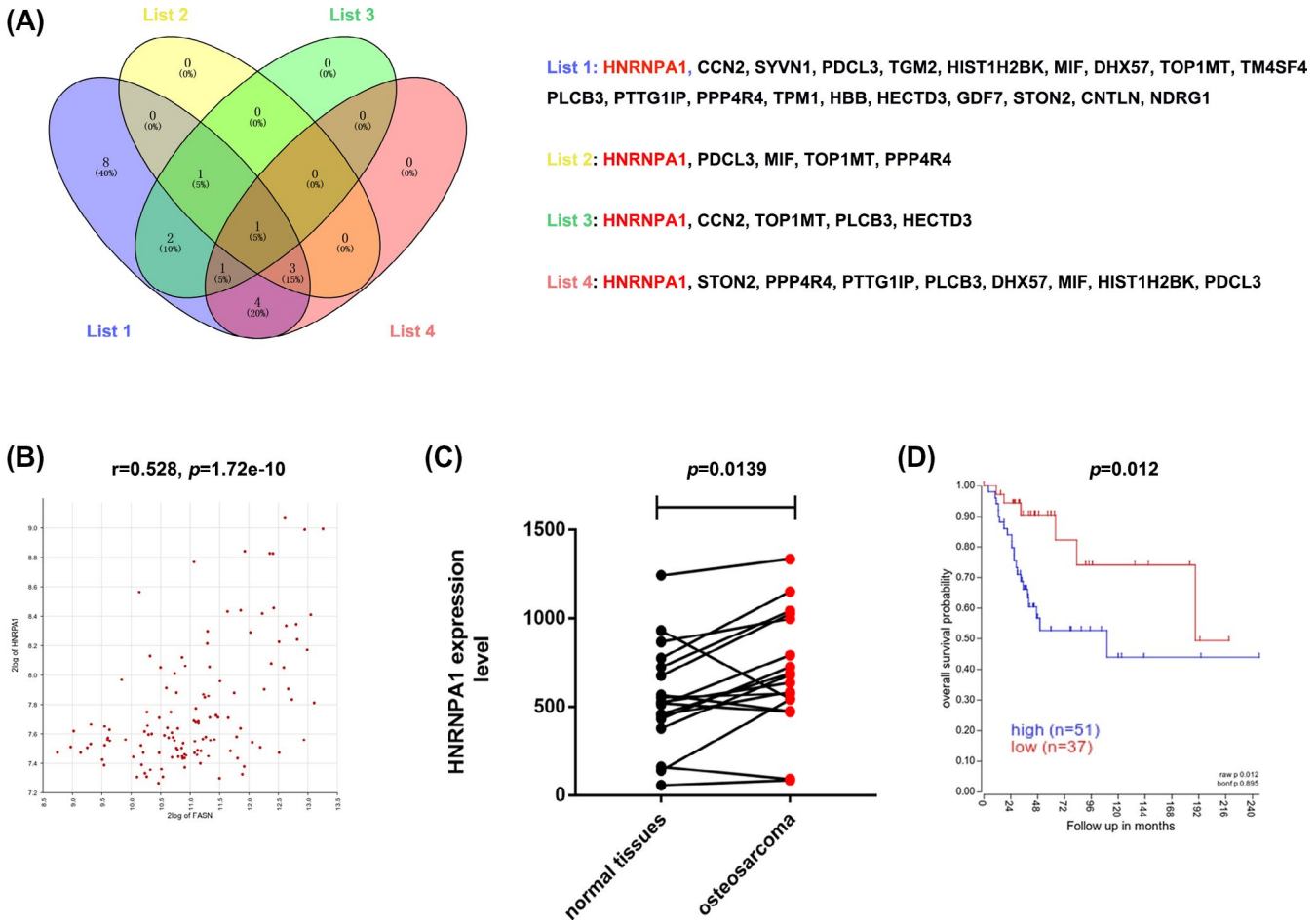

FIGURE 3 Proteomic and bioinformatic analysis identified HNRNPA1 as a FASN-regulated protein. A, Venn images revealing the overlap of target genes in the four lists. B, Pearson's correlation analysis was generated using data from 127 OS samples in R2 (https://hgserver1.amc.nl/cgi-bin/r2/main.cgi). C, HNRNPA1 expression levels were examined using data from 18 OS and paired normal tissues using the GEO (GSE99671). D, Kaplan-Meier overall survival analysis according to HNRNPA1 expression was performed based on 127 OS cases in R2 database

WB (Figure S3A,B). The results of CCK-8 assay and colony formation assay revealed that HNRNPA1 silence led to decrease in the proliferation ability and colony numbers in OS cell lines 143B and HOS (Figure 5B-D). Besides, wound-healing assay revealed that HNRNPA1 silence led to decrease of the migration ability in 143B and HOS cells (Figure 5E,F). The results of transwell migration and invasion assays showed less transmembrane cells in HNRNPA1 silence 143B and HOS cells (Figure 5G,H). In conclusion, all these results suggested that HNRNPA1 plays a tumor-promoter role in OS cells.

4 | DISCUSSION

FASN regulates the synthesis of fatty acids[17] and acts as an oncogene through its regulation of growth, migration, apoptosis, drug resistance, and radiosensitivity in tumor cells. FASN promotes cell growth and is positively regulated by PGC-1α in human colorectal cancer.[18] FASN is also upregulated in ovarian cancer cells and contributes to enhanced cell metastasis through EMT induction in vitro and in vivo.[11] In gastrointestinal stromal tumors, FASN predicts poor disease-free survival and enhances the imatinib resistance.[19] In addition, FASN inhibition promotes the sensitivity to radiation therapy in lung cancer.[10] In our previous studies, we showed that FASN-mediated anoikis resistance supports cell survival and accelerates cell metastasis in OS.[20] Despite this knowledge, the systematic description of FASN functionality in OS has not been demonstrated. Herein, we employed iTRAQ-based proteomic analysis to examine the DEPs in FASN-silenced 143B and parental cells.

In total, 567 proteins showed changes following FASN silencing. Further studies revealed that the majority of DEPs in the classification of biological functions belonged to metabolic processes, cellular processes, and biological regulation (Figure 2A), which is consistent with its functionality in fatty acid synthesis and metabolism.[5,6] Despite the lack of TF-target genes and miRNA-target gene regulatory network, KEGG pathway analysis revealed that pathways in both cancer and the ribosomes were significantly altered by FASN silence. Previous studies demonstrated that FASN regulates cancer-related pathways including NF-κβ[21] and AMPK/mTOR.[22] Of interest in this

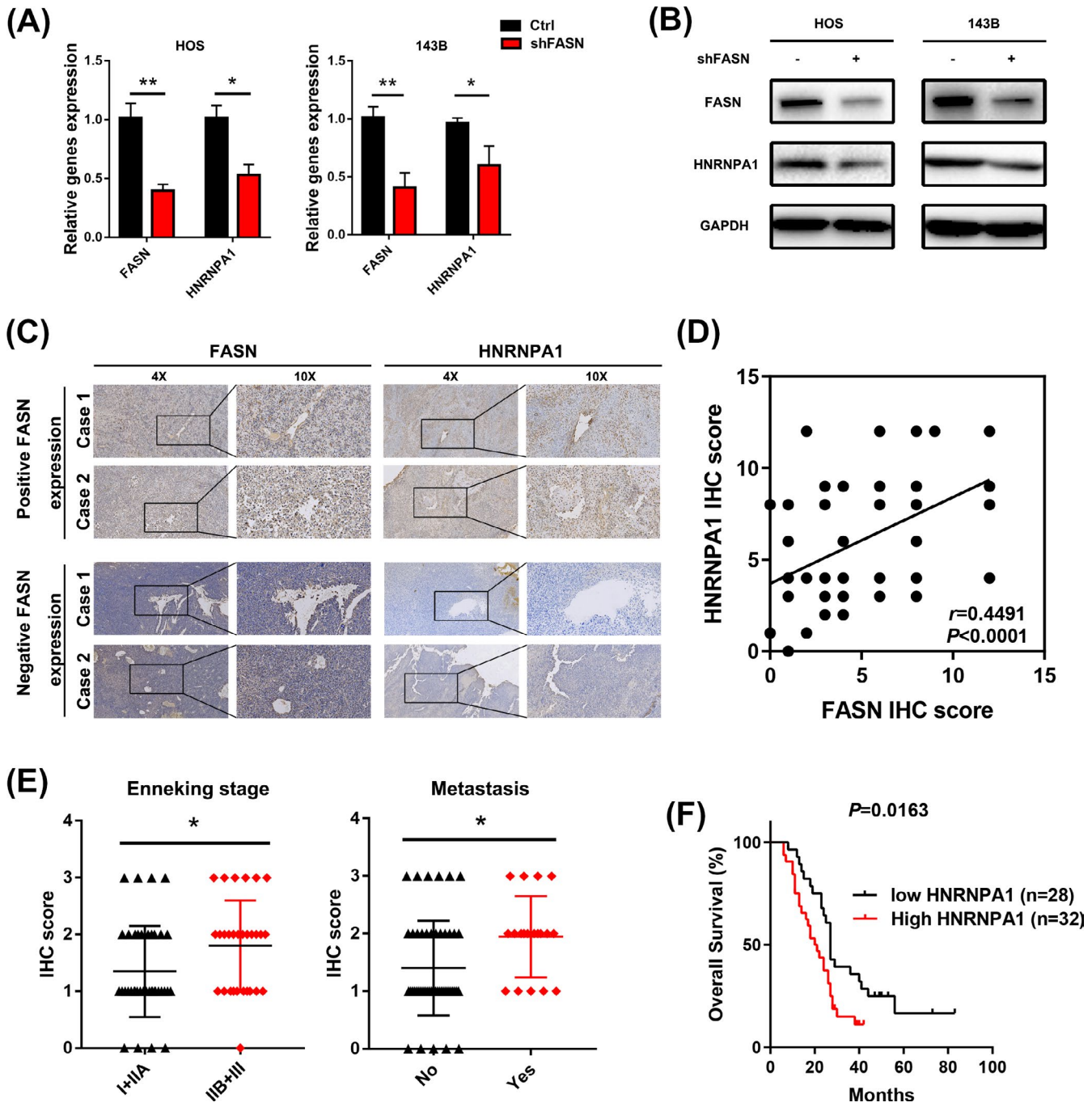

FIGURE 4 Validation of HNRNPA1 as a downstream target of FASN in OS cells and tissues. A, HNRNPA1 mRNA levels in FASN-silenced cells. B, HNRNPA1 protein levels in FASN-silenced cells. C, Representative images of FASN and HNRNPA1 immunohistochemistry staining in 71 OS samples. Scale bar: 200 μm. D, Pearson's correlation analysis between FASN and HNRNPA1 expression. E, Distribution of HNRNPA1 IHC staining scores in OS samples based on the Enneking stage and pulmonary metastasis classification. *$p < 0.05$. F, Kaplan-Meier analysis according to HNRNPA1 expression in 60 clinical OS patients

study were the changes in Ras/MAPK signaling, which is known as drivers of cell cycle progression and tumorigenesis.[23,24] Recent studies reported that FASN silence suppressed NSCLC malignancies through the inactivation of Akt/ERK signaling,[25] but reports on the regulation of Ras and MAPK signaling by FASN are sparse. Herein, our data highlight Ras/MAPK signaling as an essential feature of FASN-mediated biological processes.

FASN promotes cancer metastasis by enhancing the transcription of E-cadherin and N-cadherin and inducing EMT in ovarian cancer.[11] Besides, TGF-β is downstream of FASN and enhances the resistance to NK cell–mediated cytotoxicity by regulating the PD-L1, FASN/ TGF-β/ PD-L1 axis in NSCLC.[26] Based on iTRAQ analysis and the bioinformatic database, we identified HNRNPA1 as downstream of FASN, which was further confirmed in osteosarcoma by in vitro and IHC assays.

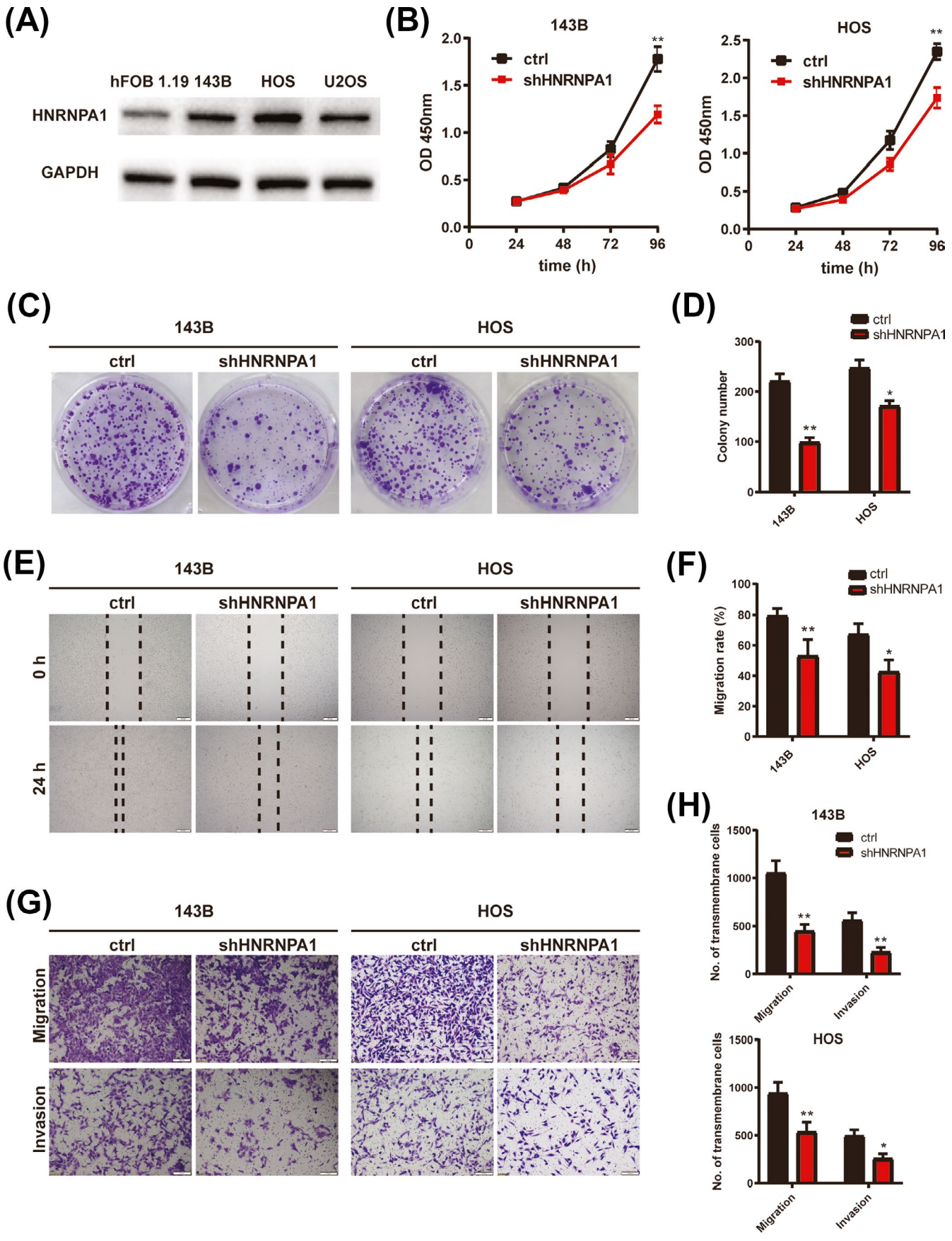
(A)
hFOB 1.19
143B
HOS
U2OS
HNRNPA1
GAPDH
(B)
143B
HOS
ctrl
shHNRNPA1
OD 450nm
time (h)
(C)
143B
HOS
ctrl
shHNRNPA1
(D)
Colony number
143B
HOS
(E)
0 h
24 h
(F)
Migration rate (%)
(G)
Migration
Invasion
(H)
No. of transmembrane cells
Migration
Invasion

FIGURE 5 HNRNPA1 silence inhibits proliferation, migration, and invasion in OS cells. A, HNRNPA1 protein level in OS cell lines. B, Quantitation of the CCK-8 assay of these transfected 143B and HOS cells. $^{**}p < 0.01$. C, Representative images of colony formation of 143B (upper panels) or HOS (lower panels) cells transfected with Lv-ctrl or Lv-shHNRNPA1 at day 8 post-infection were displayed. D, Quantitative analysis of data in C. E, Wound-healing scratch assay of 143B and HOS after transfection of either Lv-ctrl or Lv-shHNRNPA1. Cells were photographed at 0 and 24 h, and the migration rate was measured. Scale bar: 200 μm. F, Quantitative analysis of data in E. $^{*}p < 0.05$. $^{**}p < 0.01$. G, Transwell assay determined the chemotaxis of 143B and HOS cells with ctrl or HNRNPA1 silencing. Scale bar: 100 μm. H, Quantitative analysis of data in G. $^{*}p < 0.05$. $^{**}p < 0.01$

HNRNPA1 is a member of heterogeneous nuclear ribonucleoproteins and a known splicing regulator that mediates pre-mRNA processing. Abnormally expressed HNRNPA1 is observed in cervical cancer,[27] gastric cancer, and colorectal cancer [28] and has been proved to promote malignant cell behaviors. HNRNPA1 modulates apoptosis-related genes and enhances tumor growth in pancreatic cancer cells.[29] HNRNPA1 regulates tumor progression through its regulation on mRNA transcription and export. Previous studies demonstrated that HNRNPA1 modulates the pre-mRNAs of Cd44 in the inclusion of epithelial-type exons by inducing EMT in breast cancer.[30] In addition, the aberrant expression of HNRNPA1 is associated with the NF-κβ/p52/c-Myc axis [31] and the PEAK-mediated phosphorylation of HNRNPA1 accelerates HNRNPA1 degradation.[32] However, the expression and function of HNRNPA1 in osteosarcoma have not been revealed. In the present study, the correlation between HNRNPA1 expression and the prognosis of OS patients was investigated. The results suggested that HNRNPA1 is a potential functional biomarker with predictive value in OS progression. Further study revealed that HNRNPA1 is upregulated in OS cells and HNRNPA1 silence inhibits proliferation, migration, and invasion in OS cells. Despite the lack of in vivo study, our results suggest that HNRNPA1 plays a tumor-promoter role in osteosarcoma.

In summary, we highlight the new functional roles of FASN in OS progression. HNRNPA1 is downstream of FASN and acts as a biomarker and oncogene for OS. Furthermore, our data raise the possibility that the FASN/HNRNPA1 axis represents a potential therapeutic target for OS management.

CONFLICT OF INTEREST

The authors declared that they have no competing interests.

AUTHORS' CONTRIBUTIONS

DHF and SCL researched and analyzed data. DHF and JML edited the manuscript. WZC, YBZ, and XHL were responsible for clinical data collection and assay. SHH organized and design experiments.

DATA AVAILABILITY STATEMENT

In accordance with the "DFG Guidelines on the Handling of Research Data," we will make all the data available upon request. The data set will be archived for at least 10 years after publication.

ORCID

Shanhu Huang https://orcid.org/0000-0002-6977-4069

REFERENCES

1. Mirabello L, Troisi RJ, Savage SA. Osteosarcoma incidence and survival rates from 1973 to 2004: data from the surveillance, epidemiology, and end results program. *Cancer*. 2009;115(7):1531-1543.
2. Bielack S, Jurgens H, Jundt G, et al. Osteosarcoma: the COSS experience. *Cancer Treat Res*. 2009;152:289-308.
3. Moore DD, Luu HH. Osteosarcoma. *Cancer Treat Res*. 2014;162:65-92.
4. Zhang Y, Cai L, Li D, et al. Tumor microenvironment-responsive hyaluronate-calcium carbonate hybrid nanoparticle enables effective chemotherapy for primary and advanced osteosarcomas. *Nano Res*. 2018;11(9):4806-4822.
5. Alberts AW, Strauss AW, Hennessy S, Vagelos PR. Regulation of synthesis of hepatic fatty acid synthetase: binding of fatty acid synthetase antibodies to polysomes. *Proc Natl Acad Sci USA*. 1975;72(10):3956-3960.
6. Stoops JK, Arslanian MJ, Oh YH, Aune KC, Vanaman TC, Wakil SJ. Presence of two polypeptide chains comprising fatty acid synthetase. *Proc Natl Acad Sci USA*. 1975;72(5):1940-1944.
7. Ezzeddini R, Taghikhani M, Somi MH, Samadi N, Rasaee MJ. Clinical importance of FASN in relation to HIF-1alpha and SREBP-1c in gastric adenocarcinoma. *Life Sci*. 2019;224:169-176.
8. Menendez JA, Lupu R. Fatty acid synthase (FASN) as a therapeutic target in breast cancer. *Expert Opin Ther Targets*. 2017;21(11):1001-1016.
9. Lee KH, Lee MS, Cha EY, et al. Inhibitory effect of emodin on fatty acid synthase, colon cancer proliferation and apoptosis. *Mol Med Rep*. 2017;15(4):2163-2173.
10. Zhan N, Li B, Xu X, Xu J, Hu S. Inhibition of FASN expression enhances radiosensitivity in human non-small cell lung cancer. *Oncol Lett*. 2018;15(4):4578-4584.
11. Jiang L, Wang H, Li J, et al. Up-regulated FASN expression promotes transcoelomic metastasis of ovarian cancer cell through epithelial-mesenchymal transition. *Int J Mol Sci*. 2014;15(7):11539-11554.
12. Liu ZL, Mao JH, Peng AF, et al. Inhibition of fatty acid synthase suppresses osteosarcoma cell invasion and migration via downregulation of the PI3K/Akt signaling pathway in vitro. *Mol Med Rep*. 2013;7(2):608-612.
13. Song H, Liu J, Wu X, et al. LHX2 promotes malignancy and inhibits autophagy via mTOR in osteosarcoma and is negatively regulated by miR-129-5p. *Aging (Albany NY)*. 2019;11(21):9794-9810.
14. Liu X, Wang J, Gao L, Liu H, Liu C. iTRAQ-based proteomic analysis of neonatal kidney from offspring of protein restricted rats reveals abnormalities in intraflagellar transport proteins. *Cell Physiol Biochem*. 2017;44(1):185-199.
15. Liu X, Zhou Y, Lou Y, Zhong H. Knockdown of HNRNPA1 inhibits lung adenocarcinoma cell proliferation through cell cycle arrest at G0/G1 phase. *Gene*. 2016;576(2 Pt 2):791-797.
16. Chen Y, Liu J, Wang W, et al. High expression of hnRNPA1 promotes cell invasion by inducing EMT in gastric cancer. *Oncol Rep*. 2018;39(4):1693–1701.
17. Menendez JA, Lupu R. Fatty acid synthase and the lipogenic phenotype in cancer pathogenesis. *Nat Rev Cancer*. 2007;7(10):763-777.

18. Yun SH, Shin SW, Park JI. Expression of fatty acid synthase is regulated by PGC1alpha and contributes to increased cell proliferation. *Oncol Rep*. 2017;38(6):3497-3506.
19. Li CF, Fang FM, Chen YY, et al. Overexpressed fatty acid synthase in gastrointestinal stromal tumors: targeting a progression-associated metabolic driver enhances the antitumor effect of imatinib. *Clin Cancer Res*. 2017;23(16):4908-4918.
20. Sun T, Zhong X, Song H, et al. Anoikis resistant mediated by FASN promoted growth and metastasis of osteosarcoma. *Cell Death Dis*. 2019;10(4):298.
21. Chuang HY, Lee YP, Lin WC, Lin YH, Hwang JJ. Fatty acid inhibition sensitizes androgen-dependent and -independent prostate cancer to radiotherapy via FASN/NF-kappaB pathway. *Sci Rep*. 2019;9(1):13284.
22. Lu T, Sun L, Wang Z, Zhang Y, He Z, Xu C. Fatty acid synthase enhances colorectal cancer cell proliferation and metastasis via regulating AMPK/mTOR pathway. *Onco Targets Ther*. 2019;12:3339-3347.
23. Meloche S, Pouyssegur J. The ERK1/2 mitogen-activated protein kinase pathway as a master regulator of the G1- to S-phase transition. *Oncogene*. 2007;26(22):3227-3239.
24. Chambard JC, Lefloch R, Pouyssegur J, Lenormand P. ERK implication in cell cycle regulation. *Biochim Biophys Acta*. 2007;1773(8):1299-1310.
25. Chang L, Fang S, Chen Y, et al. Inhibition of FASN suppresses the malignant biological behavior of non-small cell lung cancer cells via deregulating glucose metabolism and AKT/ERK pathway. *Lipids Health Dis*. 2019;18(1):118.
26. Shen M, Tsai Y, Zhu R, et al. FASN-TGF-β1-PD-L1 axis contributes to the development of resistance to NK cell cytotoxicity of cisplatin-resistant lung cancer cells. *Biochim Biophys Acta Mol Cell Biol Lipids*. 2018;1863(3):313-322.
27. Kim YJ, Kim BR, Ryu JS, et al. HNRNPA1, a splicing regulator, is an effective target protein for cervical cancer detection: comparison with conventional tumor markers. *Int J Gynecol Cancer*. 2017;27(2):326-331.
28. Park WC, Kim HR, Kang DB, et al. Comparative expression patterns and diagnostic efficacies of SR splicing factors and HNRNPA1 in gastric and colorectal cancer. *BMC Cancer*. 2016;16:358.
29. Pham TND, Stempel S, Shields MA, et al. Quercetin enhances the anti-tumor effects of bet inhibitors by suppressing hnRNPA1. *Int J Mol Sci*. 2019;20(17):4293.
30. Moshiri A, Puppo M, Rossi M, Gherzi R, Briata P. Resveratrol limits epithelial to mesenchymal transition through modulation of KHSRP/hnRNPA1-dependent alternative splicing in mammary gland cells. *Biochimica Biophys Acta Gene Regul Mech*. 2017;1860(3):291-298.
31. Nadiminty N, Tummala R, Liu C, Lou W, Evans CP, Gao AC. NF-kappaB2/p52:c-Myc:hnRNPA1 pathway regulates expression of androgen receptor splice variants and enzalutamide sensitivity in prostate cancer. *Mol Cancer Ther*. 2015;14(8):1884-1895.
32. Koo JH, Lee HJ, Kim W, Kim SG. Endoplasmic reticulum stress in hepatic stellate cells promotes liver fibrosis via PERK-mediated degradation of HNRNPA1 and up-regulation of SMAD2. *Gastroenterology*. 2016;150(1):181 e188-193 e188.

SUPPORTING INFORMATION

Additional supporting information may be found online in the Supporting Information section.

How to cite this article: Fu D, Liu S, Liu J, et al. iTRAQ-based proteomic analysis of the molecular mechanisms and downstream effects of fatty acid synthase in osteosarcoma cells. *J Clin Lab Anal*. 2021;35:e23653. https://doi.org/10.1002/jcla.23653